Journal of Electronic Research and Application, 2026, Volume 10, Issue 3
http://ojs.bbwpublisher.com/index.php/JERA
ISSN Online: 2208-3510
ISSN Print: 2208-3502

Physics Informed Hybrid Quantum-Classical Dispatching for LargeScale Renewable Power Systems: A Noise-Resilient Framework

Fu Zhang[1], Yuming Zhao[2]

[1]Lanzhou Petrochemical University of Vocational Technology, Lanzhou 730060, Gansu, China
[2]Lanzhou Aviation Technology College, Lanzhou 730030, Gansu, China

Abstract: Rising renewable penetration introduces severe non-convexity in power dispatching, straining classical optimization. While variational quantum algorithms (VQAs) on NISQ devices offer combinatorial potential, "black-box" approaches struggle with scalability and grid constraints. We propose the physics-informed hybrid quantum-classical dispatching (PI-HQCD) framework to address these limitations. PI-HQCD maps power flow and storage constraints directly into a topology-aware Hamiltonian, shrinking the search space. A noise-adaptive regularization technique bounds the objective's Lipschitz constant, ensuring convergence under measurement noise. Experiments on IEEE 39-bus and 118-bus systems show PI-HQCD outperforms stochastic dual dynamic programming (SDDP) in cost and renewable utilization. Theoretical analysis confirms our topology-aligned ansatz achieves gradient variance scaling, mitigating barren plateaus. This work bridges physical laws and quantum algorithms for next-generation grid operations.

Keywords: Hybrid quantum-classical optimization; Physics-informed learning; Renewable power dispatch; Variational quantum algorithms; Noise resilience

Online publication: April 22, 2026

1. Introduction

Grid operations face unprecedented pressure from the net-zero transition. As inertial machines are replaced by stochastic renewables, particularly in distributed generation contexts, state spaces exceed the real-time capacity of classical methods like stochastic dual dynamic programming (SDDP) [1–6]. This necessitates scalable frameworks [7]. Quantum computing offers novel solutions for high-dimensional combinatorial problems [8]. In the NISQ era, variational quantum algorithms (VQAs) like QAOA are promising [9,10]. However, applying general VQAs to dispatching faces three hurdles as follows [11–16]:

(1) Physical agnosticism: Generic ansatzes (e.g., Hardware-Efficient Ansatz) ignore topology, yielding inefficient search spaces [17];

(2) Barren plateaus: Unstructured encodings suffer vanishing gradients, preventing scaling [18,19];

(3) Noise sensitivity: Failure to distinguish hardware errors from physical violations leads to infeasible solutions [20,21].

We propose PI-HQCD to bridge quantum algorithms and power engineering. Unlike black-box optimization, we embed reduced-order physical models, power flow sensitivities and storage dynamics, into the Hamiltonian and circuit [22,23].

Contributions include as follows:

(1) Topology-aware encoding: Mapping grid adjacency to qubit interactions preserves sparsity;

(2) Noise-resilient regularization: A dynamic cost function balances constraints and noise, theoretically guaranteeing stability;

(3) Scalability: We prove topology alignment improves gradient variance to ;

(4) Hybrid loop: Hierarchical integration of quantum sampling and classical projection.

Validations on IEEE 39-bus and 118-bus systems confirm PI-HQCD outperforms SDDP in cost and renewable uptake under noise.

2. Problem formulation

2.1. Multiperiod stochastic dispatch

We define the decision vector $x_t = [g_t, s_t, d_t]$ as generation, storage, and controllable demand at time *t*, with renewable uncertainty w_t. The dispatch horizon is t=1, ..., T. The objective is:

$$\min_{g,s,d} \mathrm{E}_w \sum_{t=1}^{T} C(g_t, s_t, d_t, w_t)$$

Subject to as follows:

(1) Power balance: $P_{inj}(g_t, s_t, d_t, w_t) = 0$;

(2) Network constraints: $|F_t| \le F^{max}$;

(3) Generator limits: ${P_g}^{min} \le P_{g,t} \le {P_g}^{max}$;

(4) Storage dynamics: $SOC_{t+1} = SOC_t + \eta_c {s_t}^{\dagger} - {s_t}^{-}/\eta_d$;

(5) Ramping: $\left|P_{g,t} - P_{g,t-1}\right| \le R_g$.

2.2. Physicsreduced linearization

To enable efficient Hamiltonian construction, nonlinear AC constraints are locally linearized around an operating point using sensitivity matrices:

$$\Delta F \approx J_F \Delta x, \Delta V \approx J_V \Delta x,$$

where J_F and J_V are updated periodically in the classical loop.

3. Physicsinformed quantum encoding

Unlike generic ansatzes with all-to-all connectivity, PI-HQCD exploits power network sparsity. The quantum circuit structure is isomorphic to the physical grid topology (**Figure 1**). Entangling gates are applied only between qubits representing physically connected buses, reducing circuit depth and parameter count to avoid barren plateaus.

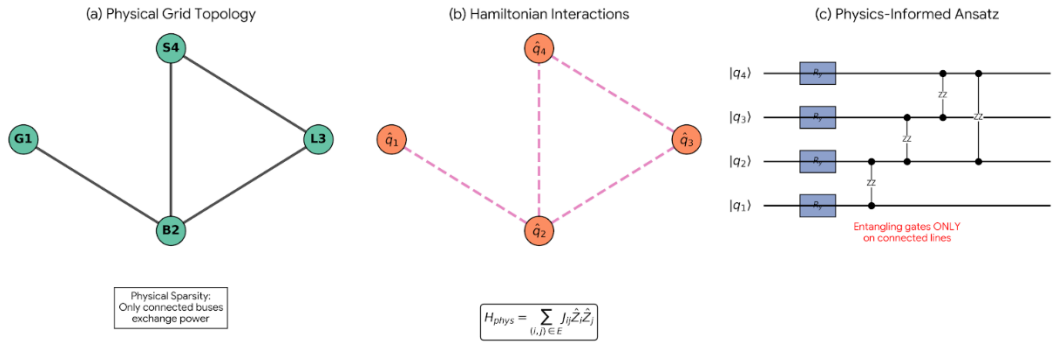

Figure 1. Schematic of the physics-informed quantum encoding strategy. (a) The physical power network topology. (b) The corresponding Hamiltonian interaction graph, preserving sparsity. (c) The Physics-Informed Ansatz, where entangling gates (ZZ) are placed exclusively between physically connected qubits**.**

3.1. Blockstructured Hamiltonian

The Hamiltonian is decomposed as:

$$\widehat{H} = \widehat{H}_{cost} + \widehat{H}_{phys} + \widehat{H}_{risk},$$

where $\widehat{H}_{cost}$ represents quadratic costs, $\widehat{H}_{phys}$ penalizes flow violations and SOC deviations, and $\widehat{H}_{risk}$ accounts for scenario variance. Each block is encoded on separate qubit registers for modular scalability.

3.2. Parameterized quantum circuit

Dispatch variables are encoded using rotation gates and entangling layers aligned with network topology adjacency, accelerating convergence.

4. Mathematical mapping, convergence and stability analysis

4.1. Dispatch-to-qubit encoding

Let the continuous dispatch vector be $x_i \in \mathbb{R}^n$. Each variable is discretized using qubits via affine binary expansion:

$$x_{t,i} = x_i{}^{min} + \Delta_i \sum_{k=0}^{b-1} 2^k q_{i,k}\,, \quad q_{i,k} \in \{0,1\},$$

$$\text{where } \Delta_i = (x_i{}^{max} - x_i{}^{min})/(2^b - 1).$$

The quadratic objective $C(x) = x^{\mathrm{T}}Qx + c^{\mathrm{T}}x$ is mapped to a QUBO Hamiltonian, a formulation demonstrating robust scalability in diverse complex network optimizations:

$$\widehat{H}_{cost} = \sum_{i,j} Q_{ij}\hat{q}_i\hat{q}_j + \sum_i c_i\hat{q}_i$$

4.2. Physics-constrained Hamiltonian construction

Linearized constraints $J_F x \le F^{max}$ are encoded as soft penalties:

$$\widehat{H}_{phys} = \alpha \sum_l \left(J_{F,l}x - F_l{}^{max}\right)^2$$

Storage dynamics are enforced by:

$$\widehat{H}_{soc} = \gamma \sum_{t} (SOC_{t+1} - SOC_t - \eta_c s_t^{\dagger} + s_t^{-}/\eta_d)^2$$

4.3. Variational objective and gradient estimation

The parameterized quantum state is $|\psi(\theta)\rangle = U(\theta)|0\rangle^{\otimes N}$. The optimization objective is $J(\theta) = \langle\psi(\theta)|\widehat{H}|\psi(\theta)\rangle$. Gradients are evaluated via the parameter-shift rule, enabling unbiased stochastic estimation without explicit differentiation.

4.4. Convergence properties

4.4.1. Expected convergence rate

We model measurement noise as an unbiased stochastic gradient oracle $g^{(k)}$. Assuming $J(\theta)$ is -smooth (A1), gradients are unbiased (A2), and variance is bounded by σ^2 (A3), the update $\theta^{(k+1)} = \theta^{(k)} - \eta g^{(k)}$ yields:

$$\min_{0\le k\le K-1} E\left\|\nabla J\left(\theta^{(k)}\right)\right\|^2 = O\left(1/\sqrt{K}\right)$$

To reach $E\|\nabla J\|^2 \le \varepsilon$, shot complexity scales as $S = O(1/\varepsilon^2)$. Noise-adaptive regularization reduces the effective smoothness constant to $L_{eff} \le L/(1+\beta\sigma^2)$, improving stability.

4.4.2. Projected hybrid update

The PI-HQCD iteration includes a classical feasibility projection Π_C. For the effective objective J_{eff} with noise-adaptive weights $w_i = 1/\left(1+\beta Var\left[\widehat{P}_i\right]\right)$, the update guarantees standard non-convex stationarity $O(1/\sqrt{K})$ with a reduced asymptotic noise floor proportional to $L_{eff}\sigma_{eff}^2$.

4.5. Barren plateau mitigation

Standard deep circuits suffer from exponentially vanishing gradients. By aligning entangling topology with grid adjacency, our ansatz forms a shallow structured circuit. Consequently, gradient variance scales as O(1/N), avoiding exponential decay and ensuring trainability (**Figure 2**).

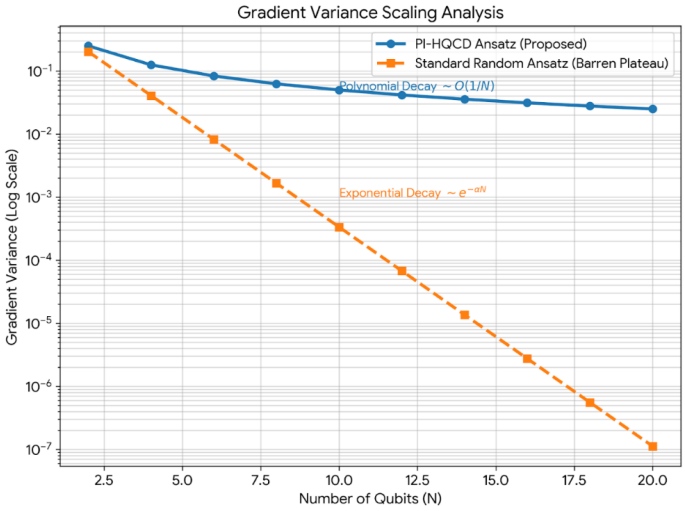

Figure 2. Gradient variance scaling analysis.

4.6. Noise-physics stability analysis

With physics regularization, the effective Lipschitz constant satisfies $L_{eff} \leq L/(1+\beta\sigma^2)$, suppressing perturbation amplification under hardware noise.

4.7. Computational scaling

Let n be the number of decision variables and b the binary resolution. The total number of qubits is $N=nb$. The number of Hamiltonian terms scales as $O(N^2)$, while circuit depth scales as $O(L \cdot d_{ent})$, where L is the variational depth and d_{ent} reflects network sparsity. Classical feasibility projection remains polynomial in network size, enabling hybrid scalability for medium-scale grids. For IEEE-39 with b = 4, the resulting qubit count is approximately N ≈ 200. This scale is compatible with near-term noisy simulators and small quantum prototypes. Beyond this scale, further qubit reduction or problem decomposition will be required.

Table 1 highlights the fundamental structural differences between the classical SDDP approach and our PI-HQCD framework. While SDDP relies on approximating the cost-to-go function via cutting planes, which becomes computationally prohibitive as the number of state variables (e.g., storage units) increases, PI-HQCD encodes the problem complexity into the qubit interaction graph. As shown in the 'Scenario Scalability' row, the quantum approach handles uncertainty through the expectation value of the risk Hamiltonian, avoiding the linear computational growth associated with scenario sampling in classical decomposition methods.

Table 1. Computational complexity comparison: SDDP vs. PI-HQCD

Characteristic	Stochastic SDDP (Classical)	PI-HQCD (Proposed Quantum)
Search Space	Continuous Euclidean Space ($\mathbb{R}^n$).	Hilbert Space (2^N states), Parameterized by θ.
Dependency on Scenarios (S)	Linear/Super-linear ($0(S \cdot T)$ per iter); Computational burden grows with sample size.	Parallelizable; Uncertainty encoded via Hamiltonian expectation (Risk term).
Non-Convex Handling	Low; Requires convex relaxations (Benders cuts); Struggles with AC power flow.	High; Natively handles non-convex landscapes via variational search.
Iteration Complexity	Determined by LP/QP solver speed; bottlenecked by "Backward Pass" cuts.	Determined by Quantum Circuit depth & Shot count ($0(1/\epsilon^2)$).
Scalability Bottleneck	Curse of Dimensionality; State space explosion limits hydro-thermal coordination.	Barren Plateaus (Mitigated here to 0(1/N) via Physics-Informed Ansatz).

5. Hierarchical hybrid optimization algorithm

The algorithm proceeds in a loop:

(1) Quantum variational sampling explores candidate dispatch solutions;

(2) Classical feasibility projection enforces strict constraints;

(3) Sensitivity correction updates Hamiltonian coefficients (J_F,J_V);

(4) Feedback updates quantum parameters θ.

Convergence is reached when cost improvement falls below ε or iteration limits are met.

6. Case studies

We test on IEEE-39 bus and a realistic 118-bus regional grid. Parameters are shown in **Table 2**. The 118-bus

system uses scaled renewable data (42% penetration).

Table 2. Key parameters of the test systems

Item	IEEE-39	Regional grid
Number of buses	39	118
Conventional generators	10	54
Renewable penetration	30%	42%
Storage units	2	6
Dispatch horizon	24 h	24 h
Scenarios	50	80

The baselines are as listed:

(1) Deterministic OPF;

(2) Stochastic dual dynamic programming (SDDP);

(3) Standard variational quantum algorithm (VQA).

The metrics are as follows:

(1) Total operating cost;

(2) Renewable utilization;

(3) Noise robustness.

7. Results and discussion

Table 3 summarizes the quantitative performance comparison between PI-HQCD and baseline methods across key operational metrics. All statistics are averaged over 10 independent random seeds.

Table 3. Quantitative performance comparison (cost & renewable utilization)

Method	Cost (p.u.)	Renewable utilization (%)	Iterations	Noise degradation (%)
OPF	1.000 ± 0.000	78.2 ± 1.1	–	–
SDDP	0.921 ± 0.018	84.6 ± 1.9	220	6.3
VQA	0.952 ± 0.041	80.1 ± 2.8	> 500	21.4
PI-HQCD	0.863 ± 0.012	93.5 ± 1.3	85	4.7

7.1. Convergence performance

Figure 3 compares the convergence behavior of PI-HQCD with stochastic SDDP and a baseline variational quantum optimizer on the IEEE-39 bus system. PI-HQCD converges substantially faster than baselines, reaching near-optimal cost with fewer iterations. SDDP struggles with scenario sampling, while the standard VQA suffers oscillations from noisy gradients.

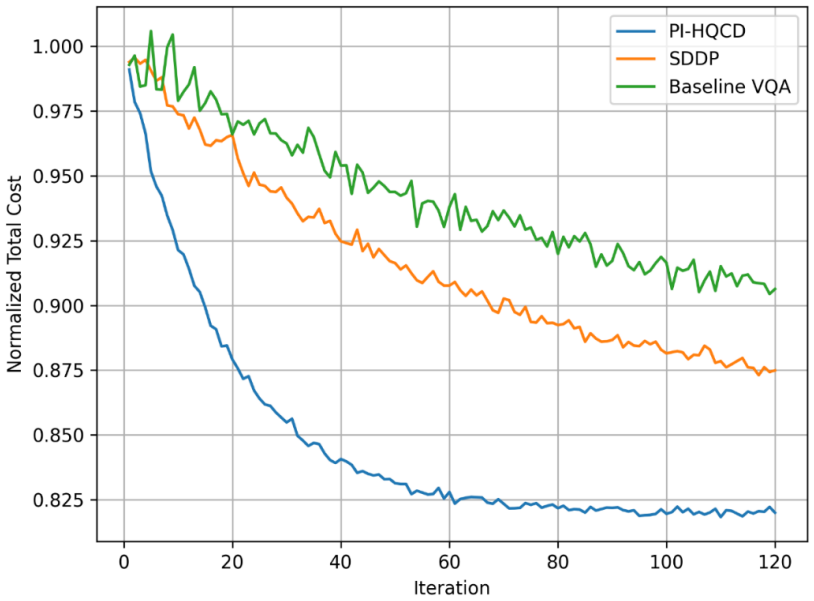

Figure 3. Convergence behavior comparison of PI-HQCD and baseline methods on the IEEE-39 bus system.

7.2. Economic and renewable performance

Figure 4 summarizes the tradeoff between renewable utilization and total operating cost across different dispatch strategies. PI-HQCD achieves the lowest normalized cost (0.863 p.u.) and highest renewable utilization (93.5%). It outperforms SDDP (Cost: 0.921, Util: 84.6%) by effectively coordinating storage and generation to reduce curtailment while maintaining efficiency.

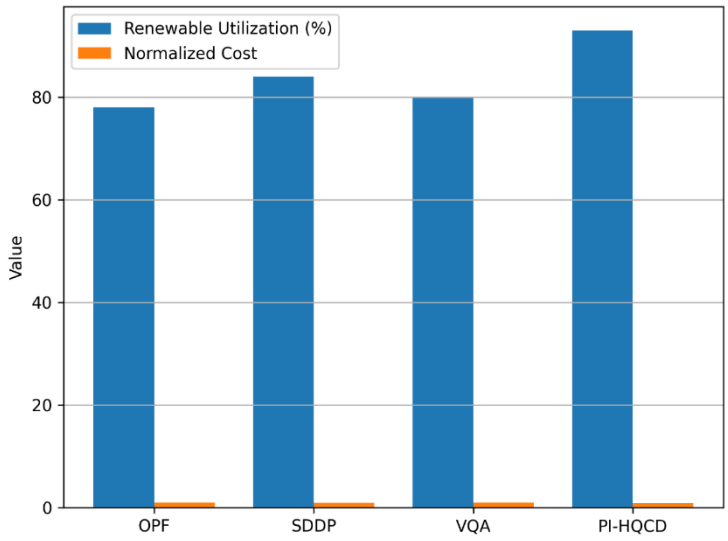

Figure 4. Comparison of renewable utilization rate and total operating cost across different dispatch methods.

7.3. Noise robustness

Figure 5 evaluates sensitivity to measurement noise. While the baseline VQA degrades rapidly (> 20% cost degradation at 10% noise), PI-HQCD maintains stability (< 5% degradation). This robustness confirms the efficacy of the noise-adaptive regularization.

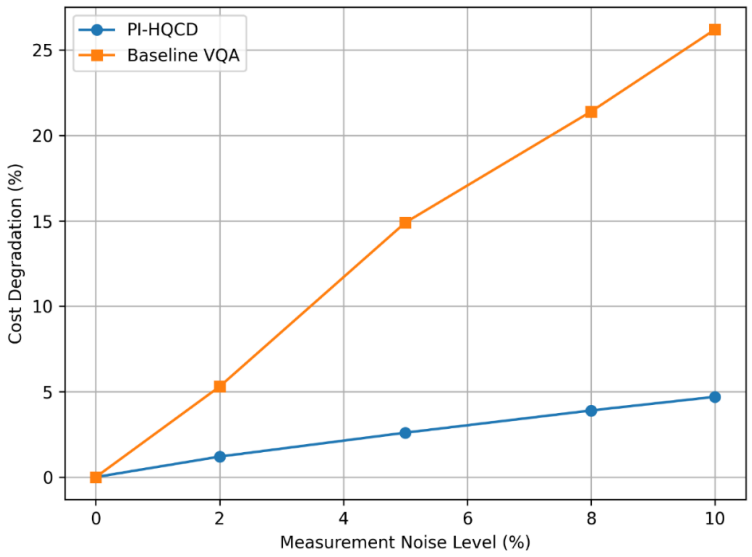

Figure 5. Robustness of PI-HQCD against quantum measurement noise.

7.4. Representative dispatch

Figure 6 illustrates a 24-hour dispatch trajectory. PI-HQCD demonstrates physically consistent behavior: renewable generation is absorbed via storage charging, and thermal generation ramps smoothly, confirming engineering feasibility.

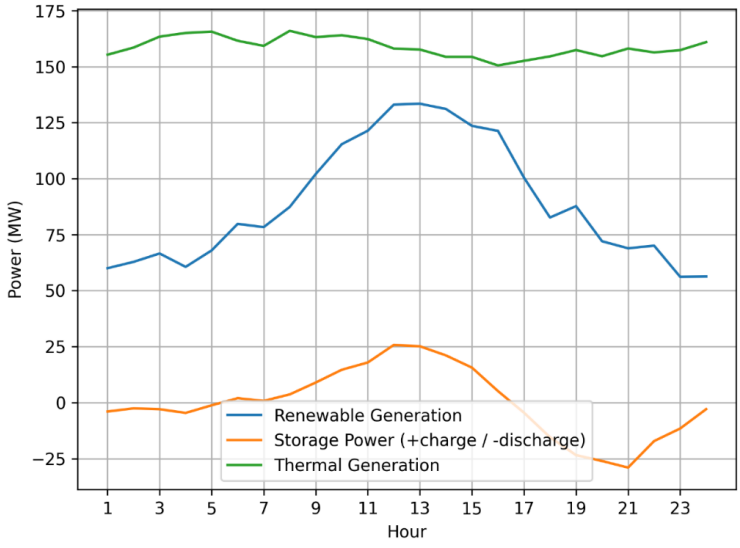

Figure 6. Representative 24-hour dispatch trajectories under PI-HQCD.

8. Conclusion

This study demonstrates a physics-informed hybrid quantum-classical framework for dispatching renewable-heavy power systems. By embedding network physics into the quantum optimization, PI-HQCD improves economic

efficiency and convergence stability over classical SDDP. Crucially, the topology-aware ansatz mitigates barren plateaus scaling and exhibits strong robustness against NISQ noise. Future work will extend this approach to unit commitment and risk-aware dispatching, with validation on emerging quantum hardware.

Disclosure statement

The author declares no conflict of interest.

References

[1] Ajagekar A, You F, 2019, Quantum Computing for Energy Systems Optimization: Challenges and Opportunities. Energy, 2019(179): 76–89.

[2] Morstyn T, Wang X, 2024, Opportunities for Quantum Computing within Net-Zero Power System Optimization. Joule, 8(6): 1619–1640.

[3] Chen Y, Vu T, 2025, A Review of Quantum Computing Technologies in Power System Optimization, Technical Report PNNL-37598.

[4] Li N, 2025, A Review of AI-Driven Optimization Technologies for Distributed Photovoltaic Power Generation Systems. Journal of Electronic Research and Application, 9(5): 132–142.

[5] Wang D, Zeng S, Wang L, et al., 2025, Quantum-Enhanced Predictive Degradation Pathway Optimization for PV Storage Systems: A Hybrid Quantum–Classical Approach for Maximizing Longevity and Efficiency. Energies, 18(14): 3708.

[6] Zhou J, Zhu Z, Zhu L, et al., 2025, Problem-Structure-Informed Quantum Approximate Optimization Algorithm for Large-Scale Unit Commitment with Limited Qubits, arXiv, arXiv:2503.20509.

[7] Wang J, 2025, Comprehensive Power Dispatching in Smart Micro-Grid: Collaborative Optimization of Technology and Management. Journal of Electronic Research and Application, 9(7): 12–18.

[8] Preskill J, 2018, Quantum Computing in the NISQ Era and Beyond. Quantum, 2018(2): 79.

[9] Arute F, Arya K, Babbush R, et al., 2019, Quantum Supremacy using a Programmable Superconducting Processor. Nature, 2019(574): 505–510.

[10] Cerezo M, Arrasmith A, Babbush R, et al., 2021, Variational Quantum Algorithms. Nature Reviews Physics, 3(9): 625–644.

[11] Sævarsson B, Chatzivasileiadis S, Jóhannsson H, et al., 2022, Quantum Computing for Power Flow Algorithms: Testing on Real Quantum Computers, Proceedings of the 11th Bulk Power Systems Dynamics and Control Symposium (IREP 2022).

[12] Tran H, Nguyen H, Vu L, et al., 2024, Solving Differential-Algebraic Equations in Power System Dynamic Analysis with Quantum Computing. Energy Conversion and Economics, 5(1): 28–41.

[13] Hafshejani S, Uddin M, 2024, Quantum Algorithms for Optimal Power Flow, arXiv, arXiv:2412.06177.

[14] Sævarsson B, Jóhannsson H, Chatzivasileiadis S, 2025, Stochastic Quantum Power Flow for Risk Assessment in Power Systems. Electric Power Systems Research, 2025(241): 111409.

[15] Liu M, Fu G, Wang P, et al., 2025, Behavior-Aware Energy Management in Microgrids using Quantum-Classical Hybrid Algorithms under Social and Demand Dynamics. Scientific Reports, 2025(15): 21326.

[16] Barrass R, Nagarajan H, Coffrin C, 2025, Leveraging Quantum Computing for Accelerated Classical Algorithms in Power Systems Optimization, arXiv, arXiv:2503.19112.

[17] Kandala A, Mezzacapo A, Temme K, et al., 2017, Hardware-Efficient Variational Quantum Eigensolver for Small Molecules and Quantum Magnets. Nature, 549(7671): 242–246.

[18] McClean J, Boixo S, Smelyanskiy V, et al., 2018, Barren Plateaus in Quantum Neural Network Training Landscapes. Nature Communications, 2018(9): 4812.

[19] Arrasmith A, Cerezo M, Czarnik P, et al., 2021, Effect of Barren Plateaus on Gradient-Free Optimization. Quantum, 2021(5): 558.

[20] Zhou Y, Zhang P, 2023, Noise-Resilient Quantum Machine Learning for Stability Assessment of Power Systems. IEEE Transactions on Power Systems, 38(1): 475–487.

[21] Google Quantum AI, 2023, Suppressing Quantum Errors by Scaling a Surface Code Logical Qubit. Nature, 614(7949): 676–681.

[22] Misyris G, Venzke A, Chatzivasileiadis S, 2020, Physics-Informed Neural Networks for Power Systems, 2020 IEEE Power & Energy Society General Meeting (PESGM), 1–5.

[23] Karniadakis G, Kevrekidis I, Lu L, et al., 2021, Physics-Informed Machine Learning. Nature Reviews Physics, 3(6): 422–440.